GEOPHYSICAL RESEARCH LETTERS, VOL. 40, 2148–2153, doi:10.1002/grl.50324, 2013

Improvement of coastal and mesoscale observation from space: Application to the northwestern Mediterranean Sea

Romain Escudier,[1,2] Jérôme Bouffard,[3,4] Ananda Pascual,[1] Pierre-Marie Poulain,[5] and Marie-Isabelle Pujol[6]

Received 22 January 2013; revised 5 March 2013; accepted 5 March 2013; published 26 May 2013.

[1] We present an innovative approach to the generation of remotely sensed high-resolution sea surface topography that improves coastal and mesoscale dynamic characterization. This new method is applied for the period 2002–2010 in the northwestern Mediterranean Sea, an area marked by a small Rossby radius. The spectral content of the new mapped data is closer to that of the along-track signal and displays higher levels of energy in the mesoscale bandwidth with the probability distribution of the new velocity fields 30% closer to drifter estimations. The fields yield levels of eddy kinetic energy 25% higher than standard altimetry products, especially over regions regularly impacted by mesoscale instabilities. Moreover, qualitative and quantitative comparisons with drifters, glider, and satellite sea surface temperature observations further confirm that the new altimetry product provides, in many cases, a better representation of mesoscale features (more than 25% improvement in correlation with glider data during an experiment). **Citation:** Escudier, R., J. Bouffard, A. Pascual, P.-M. Poulain, and M.-I. Pujol (2013), Improvement of coastal and mesoscale observation from space: Application to the northwestern Mediterranean Sea, *Geophys. Res. Lett.*, *40*, 2148–2153, doi:10.1002/grl.50324.

1. Introduction

[2] Mesoscale dynamics have significant impacts on large-scale circulation [*Lozier*, 1997] as well as on energy, heat flux transfers [*Wunsch*, 1999], and primary production [*McGillicuddy et al.*, 1998] due to important vertical exchanges associated with mesoscale features [*Pascual et al.*, 2004]. Yet, because of the difficulty of sampling mesoscale and coastal currents, which are highly variable in time and space, few observation-based studies have examined this topic.

[3] Recent advances in coastal satellite altimetry (refer to *Vignudelli et al.* [2011] for a review) have enabled dynamic signals in the 50 km coastal band to be characterized, specifically over the northwestern Mediterranean (hereinafter NWMed) [*Bouffard et al.*, 2010]. However, these studies were based on the analysis of along-track data, from which coherent structures are difficult to identify and track, and therefore, optimal mapping techniques are required. The ability to recover mesoscale data from along-track altimetry and optimally interpolate it to 2D fields is based on the merging of data of several altimeter missions [*Le Traon and Dibarboure*, 2004].

[4] The resulting altimetry maps are, however, spatially smooth and, as evidenced by previous in situ experiments [e.g., *Nencioli et al.*, 2011], lack the resolution required to detect small and coastal features (~10–100 km). *Dussurget et al.* [2011] recently addressed the need for better characterization of the mesoscale from satellite observations and developed a method that includes smaller correlation scales close to the altimeter tracks. Focusing on the Bay of Biscay, the resulting maps show coherent, finer-scale signals consistent with the information provided by remotely sensed ocean color measurements. In our study, a similar approach is adopted, but it also includes an innovative bathymetric constraint to account for the anisotropy of physical coastal features [*Huthnance*, 1995]. The methods are adapted to the NWMed, where the internal Rossby radius of deformation is four times smaller (around 10 km) than the typical value for the global ocean due to the relatively shallow thermocline (see Data S1 in the auxiliary material). The identification of mesoscale sea surface height signatures (1 cm resolution for a radius of 10 km) and the corresponding geostrophic current is particularly difficult because of the relatively low energy of the NWMed.

2. Data

2.1. Altimetry Data

[5] Eight years (2002–2010) of the standard along-track altimetry sea level anomaly data (SLA) provided by AVISO (Archiving, Validation, and Interpretation of Satellite Oceanographic data, http://www.aviso.oceanobs.com/) was used. Data from the Geosat Follow-on, Jason-1, Topex/Poseidon, Envisat, and Jason-2 satellites were included and subjected to standard geophysical corrections [*Ssalto/Duacs User Handbook*, 2012].

[6] Additionally, the regional product of merged, delayed-time gridded SLA fields ("UPD" version) for the Mediterranean Sea was also obtained from the AVISO website (details of the processing are provided in *Pujol and Larnicol* [2005]). The absolute dynamic topography (ADT), from which are derived the absolute geostrophic currents, was then calculated by adding the mean dynamic topography from *Rio et al.* [2007] to both AVISO and the generated higher-resolution SLA maps described in section 3.

Additional supporting information may be found in the online version of this article.

[1]Instituto Mediterráneo de Estudios Avanzados, IMEDEA (CSIC-UIB), Esporles, Spain.
[2]LGGE, CNRS/UJF–Grenoble 1, UMR 5183, Grenoble, France.
[3]Mediterranean Institute of Oceanography (M I O), Aix-Marseille University, Marseille, CEDEX 9, France.
[4]CNRS-INSU/IRD UM 110, Université du Sud Toulon-Var, La Garde CEDEX, France.
[5]OGS, Trieste, Italy.
[6]CLS Space Oceanography Division, Toulouse, France.

Corresponding author: R. Escudier, Instituto Mediterraneo de Estudios Avanzados, IMEDEA (CSIC-UIB), C/ Miquel Marquès, 21, 07190 Esporles, Mallorca, Spain. (romain.escudier@imedea.uib-csic.es)

0094-8276/13/10.1002/grl.50324

2.2. Auxiliary Data

[7] A bathymetry dataset [*Smith and Sandwell*, 1997] was employed to constrain the new optimal interpolation (OI) scheme in the coastal domain (see section 3 for details). To validate the methods, we perform qualitative comparisons with EUMETSAT satellite sea surface temperature (SST) provided by the O&SI SAF (www.osi-saf.org). Surface velocities from Lagrangian drifters were also used, including approximately 500 drifters covering the NWMed for the period 2002–2010 [*Poulain et al*., 2012]. The trajectories were interpolated, low-pass filtered with a cutoff at 36 h, and subsampled every 6 h to remove high-frequency components, especially tidal and inertial currents not included in the altimetry fields. Ekman velocities were removed from the drifter velocities using linear regressions with local wind products [*Poulain et al*., 2012]. Additionally, we used glider, conductivity-temperature-depth (CTD), and drifter data collected during an intensive multisensor experiment described in *Pascual et al*. [2010].

3. Methods

3.1. High-Resolution Product

[8] In order to compute the high-resolution (HR) fields, the method used is similar to that described by *Dussurget et al*. [2011]. The larger scales are obtained from the standard AVISO product (see section 2.1 for a description). Then, residuals of the along-track data are determined by subtracting these fields from the along-track raw data. Finally, an OI is performed on the residuals to obtain the finer scales. For this OI, the correlation function for the objective analysis is defined as (1)):

$$C(r,t) = e^{-\frac{r^2}{2L^2}} e^{-\left(\frac{t}{T}\right)^2} \quad (1)$$

where r and t are the spatial and time coordinates of the studied point, and L and T are the spatial and temporal correlation scales. This correlation scheme is used to determine the weights for the data interpolation. The result from the second interpolation is then added to the AVISO product to generate the high-resolution field.

3.2. Bathymetry Constraint

[9] To improve the characterization of mesoscale structures in the coastal band, where subsurface topography most likely influences their shape and propagation, we propose the addition of a bathymetry constraint with the introduction of a generalized distance that takes into account the topography (equation (2)) following the idea by *Davis* [1998] who used this approach on drifter data:

$$C(r = a - b, t) = e^{-R^2} e^{-\left(\frac{t}{T}\right)^2} \quad (2)$$

with the generalized distance R between the two points a and b defined as

$$R^2 = \frac{|a-b|^2}{2L^2} + \frac{1}{\Phi} \times \frac{|PV(a) - PV(b)|^2}{PV^2(a) + PV^2(b)} \quad (3)$$

where a and b are the two point positions, L is the correlation scale, Φ is the nondimensional parameter of the constraint, and PV is the barotropic vorticity. PV is defined as $PV = f/H$ where f represents the Coriolis parameter, and H corresponds to the bathymetry, therefore PV depends on the bathymetry. This new correlation scheme for the background error makes weights isotropic in the center of the basin where the bottom is relatively flat and elongated along the topography where there are strong bathymetry gradients, thereby maintaining the offshore gradients of the coastal features. The new fields are hereinafter referred to as HR + bathy.

[10] To adjust the OI parameters, sensitivity tests based on Monte Carlo analyses were performed. The values that optimize the signal-to-noise ratio were $L = 30$ km, $T = 3$ days, and $\Phi = 0.7$, with a measurement error variance of 3 cm^2.

4. Results

4.1. Spectra

[11] The spatial power spectra densities of SLA (Figure 1) show a significant discrepancy between the original along-track signal and AVISO fields for spatial scales smaller than 150 km. For scales between 50 and 100 km, an increase in energy in the HR products is observed, which agrees with the along-track spectrum. Concerning the wavenumber spectrum slopes, the HR product ($k^{-2.8}$) is closer to the along-track data ($k^{-2.5}$) than the AVISO product ($k^{-3.7}$) in the 70–200 km band. Because noise tends to weaken the slope [*Xu and Fu*, 2012], the along-track slope may be underestimated. Nevertheless, the HR field slopes are much closer to the along-track slope than the AVISO slope, indicating a more coherent statistical representation of the geostrophic turbulent cascade.

4.2. Statistics on Geostrophic Currents

[12] A direct comparison between collocated drifter and altimetric velocities is difficult because a slight displacement of small-scale features can induce a drastic change in the drifter trajectory that will not be captured by the altimetry coverage. Therefore, a statistical approach using statistical distributions (probability density functions) was employed for the entire 8 year period to quantitatively evaluate the performance of different remotely sensed products. When compared to the drifter distribution, the HR product distribution shows a better agreement than the AVISO distribution (refer to the histogram in Figure S2 in the auxiliary material). The distribution was improved in terms of root mean square differences (RMSDs) by 28% (HR) and 30% (HR + bathy), confirming a significant enhancement of the statistical characterization of mesoscale dynamics in the NWMed.

4.3. Spatial Distribution of Eddy Kinetic Energy

[13] Figure 2 presents the 8 year mean eddy kinetic energy (EKE) derived from the SLA of the different 2D mapping methods, as well as the one obtained from the drifter velocities. As observed by *Poulain et al.,* [2012], the significant difference in the magnitude of EKE between altimetry products and drifters could be attributed to ageostrophic motions and/or nonuniform sampling in space and time of drifter trajectories. Nevertheless, the spatial distribution of high EKE patterns is similar in the drifter-based and altimetry-based EKE maps with high values between Menorca and Sardinia and lower values in the north. The HR products, both with and without the bathymetric constraint, exhibit a higher-average EKE (approximately 50 cm^2/s^2) than the AVISO product. Furthermore, this increase is not homogeneously distributed and appears more substantial in the Balearic

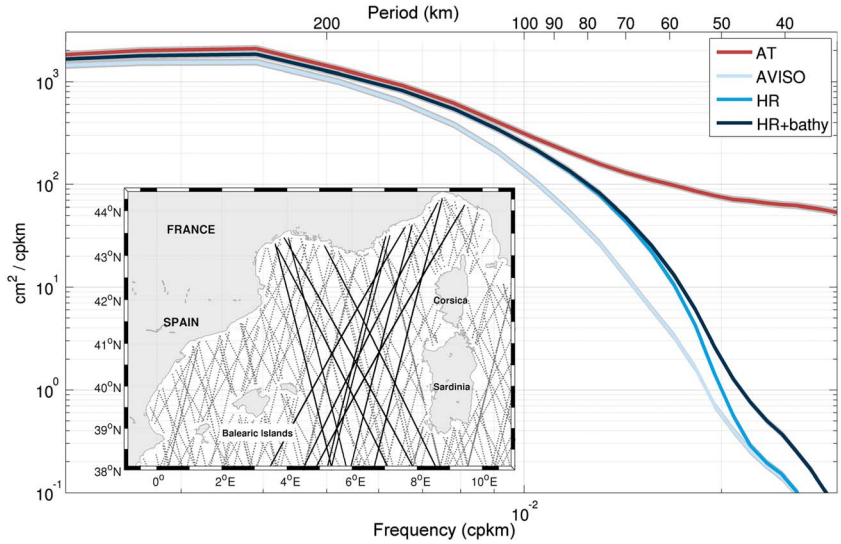

Figure 1. The mean power spectra of the SLA in the NWMed for the different products, with the 95% confidence interval shaded in gray (error was estimated using chi-square test). In dark red is the along-track 1 Hz data while the gridded fields are in blue, the lighter being the AVISO product and the darker ones are the HR products. The spectrum for these datasets was computed from SLAs interpolated at the track locations. The fitted slopes between 70 and 250 km are indicated for each spectrum. Bottom left corner: map with the position of the tracks (the long tracks used for the spectra computation are shown in black, and the others are shown in gray).

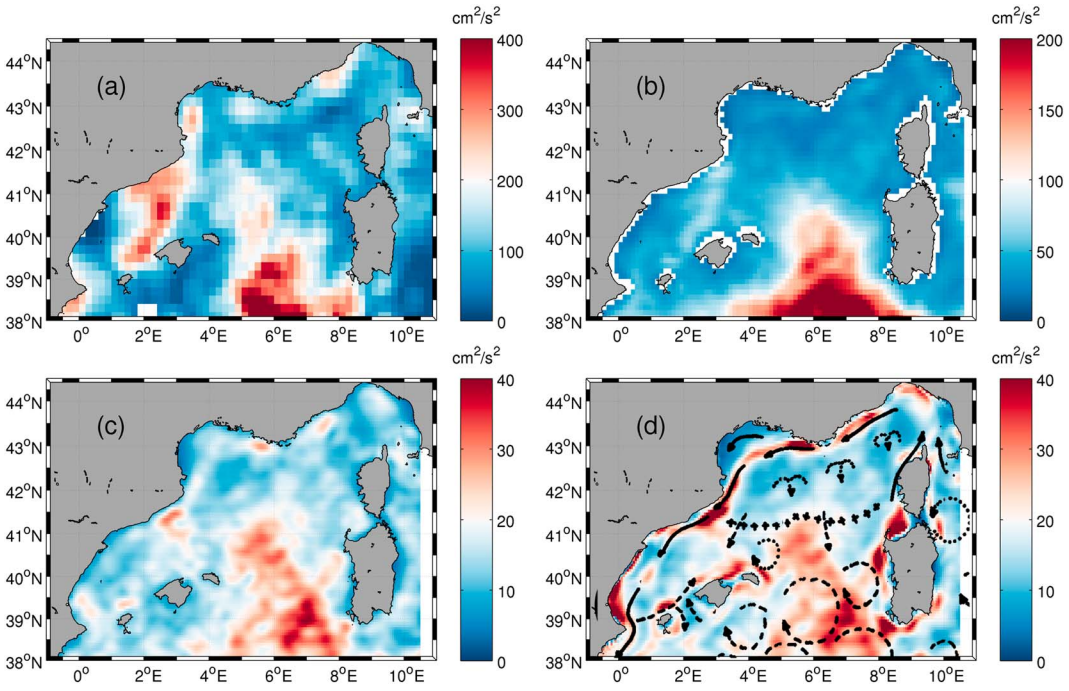

Figure 2. Eddy kinetic energy over the period 2003–2010. The top panels are the mean values over this period obtained from the (a) drifters and the (b) AVISO maps. The bottom panels show the difference between the (c) HR or (d) HR + bathy and AVISO. For the drifter map, the EKE is calculated from the drifter geostrophic velocity anomalies, obtained by subtracting the mean velocity computed in each bin of size 0.2° × 0.2° from the velocity measured by the drifters. The circulation scheme established by *Millot* [1999] is superposed on Figure 2d. The symbol meanings are as follows: continuous arrows are steady paths, dashed arrows are mesoscale currents throughout the year, and dashed circles are wind-induced mesoscale.

Sea, along the southern coast of France and in the center of the basin where the EKE from drifters is also high. As expected, the HR + bathy product reveals stronger EKE near the coast and in areas where several previous studies (including *Millot* [1999]) (see Figure 2d in this article) have shown a relative strong mesoscale activity because of Northern and Balearic slope current instabilities, which regularly form meanders and eddy-like structures [*Bouffard et al.*, 2010].

4.4. Focus on Specific Events

[14] A coastal mesoscale event observed during a multiplatform experiment (Sistema Integrado de Oceanografía Operacional, SINOCOP) illustrates the performance of the methods (Figure 3). The analysis of the collected in situ data revealed the presence of a small-scale anticyclonic eddy (~25 km diameter) on the northern shore of Mallorca (Figure 3a). This structure blocked the usual path of the Balearic Current along the coast, deflecting the main north-eastward flow to the north. Drifter data provide horizontal velocities associated with the eddy on the order of 20 cm/s [*Pascual et al.*, 2010].

[15] As shown in Figure 3b, AVISO altimeter maps were unable to correctly reproduce the southern recirculation of the small-scale anticyclonic eddy. The statistics presented in Table 1 reveal that the correlations, as well as the RMSDs with respect to drifter-derived currents, are significantly better for the HR method (improvements > 10%). Despite these improved statistics (cf. Figures 3c and 3b), the HR method does not perform very well near the coast. When the bathymetric constraint is used, a more accurate representation of the eddy is obtained, both qualitatively (Figure 3d) and statistically (Table 1). The eddy is then almost perfectly collocated with the drifter trajectory, and the HR + bathy-derived currents agree with the drifter velocities, with a correlation of 0.94 and an RMSD below 7 cm/s (i.e., close to the statistical results obtained from comparisons between gliders and drifters; see Table 1).

[16] Qualitative comparisons between satellite SST and altimetry-derived currents are also performed to evaluate the HR + bathy method. For this, we focused on the Balearic Sea which is a particular frontal area where SST gradients, used here as a tracer, allow us to clearly identify mesoscale features arising from frontal dynamics. We looked at the first 6 months of 2009, before and after the SINOCOP experiment. Confirming the previous statistical results, we found several cases of frontal dynamical structures detected both by the satellite SST and the HR + bathy product but not reproduced by AVISO (Figure 4; another example is provided for 2010 in Figure S3). The relatively low number of examples is due to cloud coverage and the fact that the new method, in most cases, only induces changes in the current intensity and not in the shape of dynamical small-scale features. For this reason, SST cannot be used to perform a quantitative

Table 1. Statistical Results Obtained From Comparisons Between Gliders and Drifters[a]

	Glider	AVISO	HR	HR + Bathy
R-U	0.92	0.59	0.84	0.96
R-V	0.76	0.77	0.87	0.94
RMSD-U (cm/s)	9.0	12.0	10.0	7.0
RMSD-V (cm/s)	2.9	7.0	6.2	4.9

[a]Diagnostics for the experiment are shown in Figure 3. The top two lines show the correlation (*R*) between the different estimated product velocities (from gliders, AVISO maps, and the two new HR fields) and the drifter-derived velocities, while the last two rows show the root mean square difference (RMSD) between the two velocities. Note that all correlations are significant at the 95% confidence level.

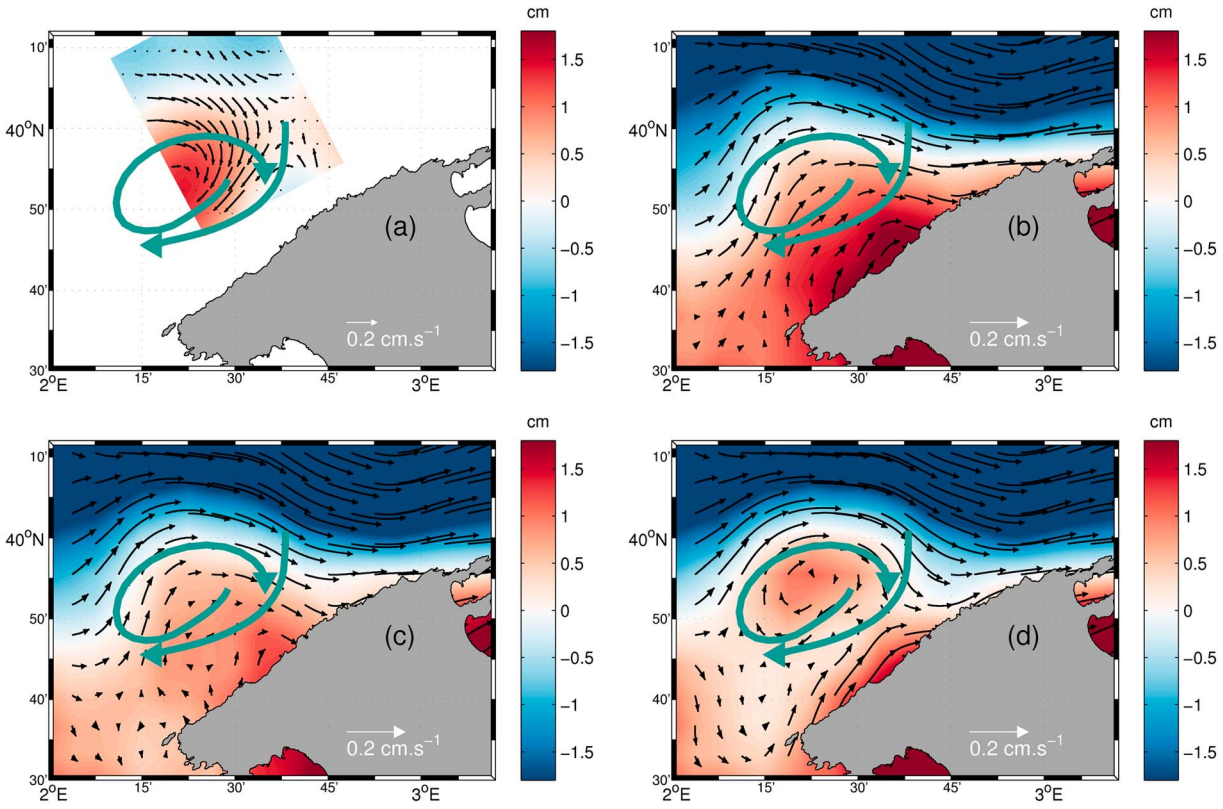

Figure 3. Multisensor experiment north of Mallorca (14 May 2009): (a) The dynamic height computed from spatially interpolated glider and CTD temperature and salinity fields. The ADT overlapped by the derived geostrophic current from the (b) AVISO, (c) HR, and (d) HR + bathy fields on the same date. The green lines are the filtered trajectories of two drifting buoys launched at the same time.

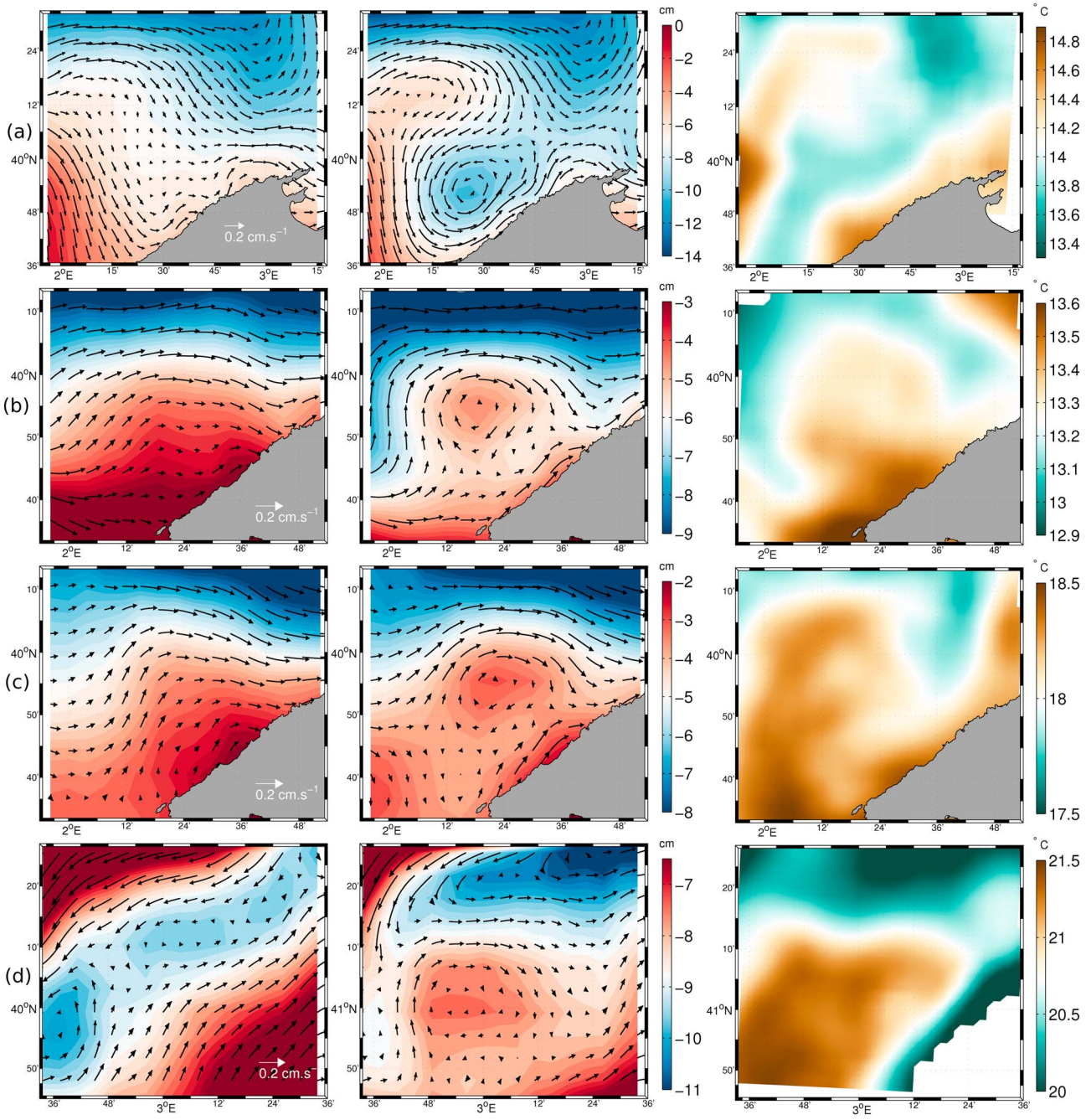

Figure 4. Comparisons between the different altimetric products (SSH in centimeter + geostrophic current) and satellite SST in degrees Celsius in the Catalan and Balearic Sea for different periods of 2009. The first column features the AVISO standard product, the second the HR + bathy product (equivalent results are obtained with HR, but to a lesser extend), and the last one the SST, filtered at 15 km, from EUMETSAT. The dates for each snapshot are respectively 19 January (row a, SST observation of a dipole eddy structure), 23 February (row b, SST observation of a cyclonic coastal eddy), 14 May (row c, SST observation of the SINOCOP eddy), and 6 June 2009 (row d, SST observations of a thermal front separated by a zonal jet).

diagnostics since no simple relation exists between SST gradients and the geostrophic current intensity.

5. Discussion

[17] Despite the promising results shown in the previous sections, it is, however, fundamental to have in mind that the coastal and mesoscale characterizations from existing observations directly depend upon altimeter track availability, as illustrated in Figure S4 (auxiliary material) showing the error field estimated from the OI for the SINOCOP period. In this figure, it appears that between tracks (left panel) or between satellite cycle (right panel), the fine-scale interpolation does not add relevant information. The interpolation could then create spurious eddies in these areas by extrapolating short-lived eddies in time or if the bathymetry constraint is poorly parameterized. These limitations also make the long-term tracking of small-scale dynamical features difficult, which will require the use of a denser satellite constellation or complementary measurements to reduce the OI mapping error.

[18] Nevertheless, with regard to the results obtained, a small coastal eddy in the north of Mallorca seems to appear regularly in the new data and has been confirmed by SST and drifter data in some cases. The detection and study of such small structures is crucial for evaluating transport variability [*Pinot et al*., 1995].

6. Conclusions

[19] In this study, alternative methods to generate high-resolution altimeter maps were developed and evaluated both quantitatively and qualitatively. These methods employ the standard altimeter gridded products as a first guess, and subsequently, an optimal interpolation is performed on the along-track raw data with the aim of resolving features at smaller scales. The optimal interpolation can be isotropic (HR), or a bathymetric constraint can be applied to the OI in order to improve the characterization of coastal structures (HR + bathy). These methods are tested in the NWMed.

[20] The new mapping methods demonstrated herein have enabled the detection of new coherent dynamical structures. In addition, when compared to AVISO, they improve the coherence of the spectral content with respect to along-track data and the velocity statistical distribution by 30%. The new fields also display smaller features with realistic higher levels of EKE of about 25%. In addition, the obtained results agree with sea surface temperature, drifter, and glider observations, specifically in areas where relatively intense mesoscale activity was previously observed and/or simulated. Such data could therefore be used to study some specific events, especially during cruise campaigns operating in the neighborhood of altimetric track passages.

[21] Standard along-track data have been used in order to assess the performance of the method. Yet, as several upgraded coastal along-track products are available (such as X-TRACK or PISTACH), they could be used to improve the performance in coastal zones. Furthermore, the new method described in this paper will benefit from an increased number of satellite missions (AltiKa in 2013 and Sentinel 3 in 2014) and the combination with regular in situ measurements (e.g., Argo floats and gliders) paving the way for promising improvements in coastal mesoscale observation.

[22] **Acknowledgments.** R. Escudier has a JAE CSIC predoctoral fellowship. The altimeter products used in this study were produced by SSALTO-DUACS and distributed by AVISO with support from CNES. We are thankful for the contributions of B. Garau, M. Martínez-Ledesma, and K. Sebastian during the data acquisition and processing from gliders and drifters in the Balearic Sea. We also thank M. Menna, R. Gerin, and A. Bussani for processing the drifter data for the northwestern Mediterranean Sea. This work was partially funded by the MyOcean2 EU FP7 project.

References

Bouffard, J., A. Pascual, S. Ruiz, Y. Faugère, and J. Tintoré (2010), Coastal and mesoscale dynamics characterization using altimetry and gliders: A case study in the Balearic Sea, *J. Geophys. Res.*, *115*, C10029, doi:10.1029/2009JC006087.

Davis, R. E. (1998), Preliminary results from directly measuring middepth circulation in the tropical and South Pacific, *J. Geophys. Res.*, *103*(C11), 24,619–24,639.

Dussurget, R., F. Birol, R. Morrow, and P. De Mey (2011), Fine resolution altimetry data for a regional application in the Bay of Biscay, *Mar. Geodesy*, *34*, 3–4, 447–476, http://dx.doi.org/10.1080/01490419.2011.584835

Huthnance, J. M. (1995), Circulation, exchange and water masses at the ocean margin: The role of physical processes at the shelf edge, *Progr. Oceanogr.*, *35*, 353–431.

Le Traon, P. Y., and G. Dibarboure (2004), An illustration of the unique contribution of the TOPEX/Poseidon – Jason-1 tandem mission to mesoscale variability studies, *Mar. Geodesy*, *27*, 3–13.

Lozier, M. S. (1997), Evidence for large-scale eddy-driven gyres in the North Atlantic, *Science*, *277*(5324), 361–364.

McGillicuddy, D. J., A. R. Robinson, D. A. Siegel, H. W. Jannasch, R. Johnson, T. D. Dickey, J. McNeil, A. F. Michaels, and A. H. Knap (1998), Influence of mesoscale eddies on new production in the Sargasso Sea, *Nature*, *394*(6690), 263–266.

Millot, C. (1999), Circulation in the western Mediterranean Sea, *J. Mar. Syst.*, *20*(1–4), 423–442.

Nencioli, F., F. d'Ovidio, A. M. Doglioli, and A. A. Petrenko (2011), Surface coastal circulation patterns by in-situ detection of Lagrangian coherent structures, *Geophys. Res. Lett.*, *38*, L17604, doi:10.1029/2011GL048815.

Pascual, A., D. Gomis, R. L. Haney, and S. Ruiz (2004), A quasigeostrophic analysis of a meander in the Palamos Canyon: Vertical velocity, geopotential tendency, and a relocation technique, *J. Phys. Oceanography*, *34*(10), 2274–2287.

Pascual, A., S. Ruiz, and J. Tintoré (2010), Combining new and conventional sensors to study the Balearic Current, *Sea Technol.*, *51*(7), 32–36.

Pinot, J. M., J. Tintoré, and D. Gomis (1995), Multivariate analysis of the surface circulation in the Balearic Sea, *Prog. Oceanography*, *36*(4), 343–376.

Poulain, P.-M., M. Menna, and E. Mauri (2012), Surface geostrophic circulation of the Mediterranean Sea derived from drifter and satellite altimeter data, *J. Phys. Oceanogr.*, *42*, 973–990, doi:http://dx.doi.org/10.1175/JPO-D-11-0159.1.

Pujol, M., and G. Larnicol (2005), Mediterranean sea eddy kinetic energy variability from 11 years of altimetric data, *J. Mar. Syst.*, *58*(3–4), 121–142, 11.

Rio, M.-H., P. M. Poulain, A. Pascual, E. Mauri, G. Larnicol, and R. Santoleri (2007), A mean dynamic topography of the Mediterranean Sea computed from altimetric data, in situ measurements and a general circulation model, *J. Mar. Syst.*, *65*(14), 484–508.

Smith, W. H. F., and D. T. Sandwell (1997), Global sea floor topography from satellite altimetry and ship depth soundings, *Science*, *277*(5334), 1956–1962.

Ssalto/Duacs User Handbook (2012): (M)SLA and (M)ADT near-real time and delayed time products SALP-MU-P-EA-21065-CLS, edition 2.9, February.

Vignudelli, S., A. Kostianoy, P. Cipollini, J. Benveniste (eds.) 2011, Coastal altimetry, Springer, 1st Edition., 2011, XII, 566 p. 216 illus., 186 inc color, doi:10.1007/978-3-642-12796-0.

Wunsch, C. (1999), Where do ocean eddy heat fluxes matter?, *J. Geophys. Res.*, *104*(C6), 13,235–13,249.

Xu, Y., and L.-L. Fu (2012), The effects of altimeter instrument noise on the estimation of the wavenumber spectrum of sea surface height, *J. Phys. Oceanography* 120822104910002.